

# Implementations of the finite element method for the collective model of atomic nuclei

Gusev A.A. (JINR, Dubna, Russia)

in collaboration with:

**Statement of the problem:** Derbov V.L. (SSU, Saratov, Russia),  
Deveikis A. (VMU, Kaunas, Lithuania) Hess P.O.(UNAM, Mexico, Mexico),

Mardyban E.V., Vinitisky S.I.(JINR, Dubna, Russia),

**Implementations:** Blinkov Yu.A. (SSU, Saratov, Russia),  
Buša J. Jr., Chuluunbaatar G., Chuluunbaatar O. (JINR, Dubna, Russia)

## Outline

- Introduction
- Formulation of BVP and GTM and FEM schemes
- BVP for five-dimensional quadrupole Hamiltonian model
- Benchmark calculations of  $^{154}\text{Gd}$  and  $^{238}\text{U}$  in the RMF model
- Conclusions

October 24, 2024

Mathematical Modeling and Computational Physics, 2024, Yerevan, Armenia

## Introduction: Recalling

### Finite element methods (FEM)

- Kumar, K. and Baranger, M.: Complete numerical solution of Bohr's collective Hamiltonian, Nucl. Phys. A 92, 608–652 (1967).
- Troltenier, D., Maruhn, J. A., Greiner, W., and Hess, P. O.: A general numerical solution of collective quadrupole surface motion applied to microscopically calculated potential energy surfaces, Z. Phys. A – Hadrons and Nuclei 343, 25–34 (1992).
- Batgerel, B., Blinkov, Yu.A., Vinitsky, S.I., Gusev, A.A., Chuluunbaatar, O., Deveikis, A., Buša Jr., J., Chuluunbaatar, G., and Ulziibayar, V.: Schemes of finite element method for solving multidimensional boundary value problems, J. Math. Sci., New York 279, 738 (2024)

### Galerkin methods (GTM) single or double basis sets for single or double wells

- Hess, P.O., Seiwert, M., Maruhn, J., and Greiner, W.: General collective model and its application to  ${}_{92}^{238}\text{U}$ , Z. Phys. A – Atoms and Nuclei 296, 147-163 (1980)
- Troltenier, D., Maruhn, J. A., and Hess, P. O.: Numerical application of the geometric collective model, In: Langanke, K., Maruhn, J.A., Konin, S.E. (eds.) Computational Nuclear Physics 1, 105–128, Springer-Verlag, Berlin (1991)
- Libert, J., Girod, M., and Delaroche, J.-P. L.: Microscopic descriptions of superdeformed bands with the Gogny force: Configuration mixing calculations in the  $A \sim 190$  mass region, Phys. Rev. C 60, 054301-1–26 (1999).
- Delaroche, J.-P., Girod, M., Goutte, H., Libert, J.: Structure properties of even-even actinides at normal and super deformed shapes analysed using the Gogny force, Nucl. Phys. A 771, 103–168 (2006)
- J. Libert, J.-P. Delaroche, and M. Girod, Five-dimensional collective Hamiltonian with the Gogny force: An ongoing saga. Eur. Phys. J. A (2016) 52: 197

## Formulation of BVP and GTM and FEM schemes

### Self-adjoint BVP for the elliptic differential equation

$$(T+V(x)-E)\Phi(x)=0, \quad T=-\frac{1}{g_0(x)}\sum_{i,j=1}^d\frac{\partial}{\partial x_i}g_{ij}(x)\frac{\partial}{\partial x_j}, \quad \mathbf{x}=(x_1,\dots,x_d)\in\Omega\in\mathcal{R}^d, \quad (1)$$

$$g_0(x) > 0, \quad g_{ji}(x) = g_{ij}(x), \quad + \text{Neumann or Dirichlet boundary conditions.} \quad (2)$$

### The expansion over the appropriate basis functions $N_l(x)$

in the Galerkin type method (GTM), or finite element method (FEM)

$$\Phi_m^h(x) = \sum_{l=1}^{L_\Omega} N_l(x)\Phi_{lm}^h. \quad (3)$$

### Algebraic generalized eigenvalue problem

$$(\mathbf{A} - \mathbf{B}E_m^h)\Phi_m^h = 0, \quad (\Phi_m^h)^T \mathbf{B}\Phi_m^h = 1, \quad (4)$$

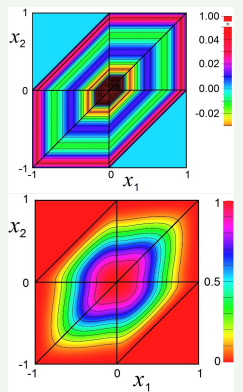
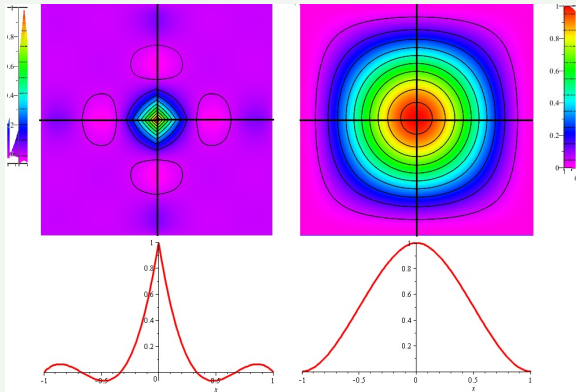
with respect to  $E_m^h$  and  $\Phi_m^h$ .

In the FEM, the polyhedral domain  $\bar{\Omega}$  is divided into subdomains  $\Delta_q$ , called finite elements  $\bar{\Omega} = \bar{\Omega}_h(x) = \bigcup_{q=1}^Q \Delta_q$ ,  $\bar{\Omega} \subset \mathcal{R}^d$ .

The local basis functions, LIPs or HIPs are introduced:  $\hat{\varphi}_{rq}^{\kappa}(x)$ ,  $x \in \Delta_q$ .

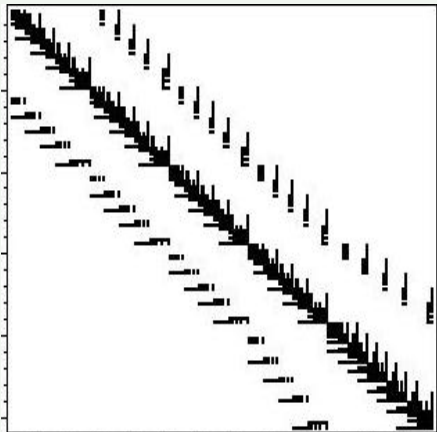
The piecewise polynomial functions (PPFs) constructed by joining the polynomials  $\hat{\varphi}_{rq}^{\kappa p'}(x)$  on the finite elements  $\Delta_q \in \bar{\Omega}_h(x)$

$$N_l(x) = \bigcup_{q=1}^Q \{\hat{\varphi}_{rq}^{\kappa}(x) | x \in \Delta_q\}. \quad (5)$$

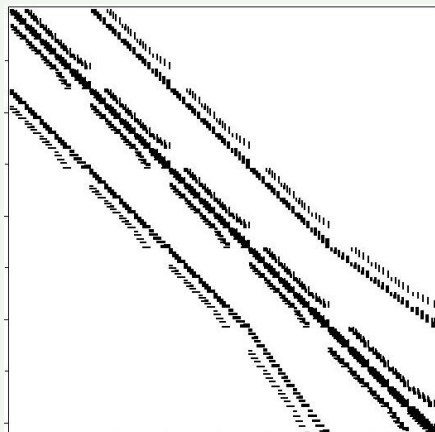


# Structures of mass and stiffness matrices A and B

2D



3D



## 5DBVP for the five-dimensional quarupole Hamiltonian(5DQH)

The Schrödinger equation with respect to eigenfunction  $\Psi_{nIM} \equiv \Psi_{nIM}(\beta, \gamma, \vartheta_i)$  and the corresponding eigenvalues of energy  $E_{nl}$  has the form

$$\frac{2}{\hbar^2}(\hat{H} - E_{nl})\Psi_{nIM} = \left( \hat{T}_{\text{vib}} + \hat{T}_{\text{rot}} + \frac{2}{\hbar^2}(V - E_{nl}) \right) \Psi_{nIM} = 0. \quad (6)$$

orthogonality and normalization conditions

$$\int_{\Omega_5} \Psi_{nIM} \Psi_{n'I'M'} g_0(\beta, \gamma) d\beta d\gamma \sin \vartheta_2 d\vartheta_1 d\vartheta_2 d\vartheta_3 = \delta_{nn'} \delta_{II'} \delta_{MM'}. \quad (7)$$

The eigenfunction  $\Psi_{nIM}$  in the representation of the angular momentum  $l$  and its projections  $K$  and  $M$  on the third axes of the intrinsic and laboratory frames

$$\Psi_{nIM}(\beta, \gamma, \vartheta_i) = \sum_{K \geq 0, \text{even}}^l D_{MK}^{l*}(\vartheta_i) \Phi_{nlK}(\beta, \gamma), \quad (8)$$

where  $D_{MK}^{l*}(\vartheta_i)$  are the normalized D-functions with the space parity  $\hat{\pi} = \pm 1$

$$D_{MK}^{l*}(\vartheta_i) = \sqrt{\frac{2l+1}{8\pi^2}} \frac{(D_{MK}^{l*}(\vartheta_i) + \hat{\pi}(-1)^l D_{M-K}^{l*}(\vartheta_i))}{\sqrt{2(1 + \delta_{K0})}}. \quad (9)$$

## 2DBVP for five-dimensional quarupole Hamiltonian(5DQH)

The unknown set of  $l_{\max}$  internal components  $\Phi_{nlK} \equiv \Phi_{nlK}(\beta, \gamma)$ , where  $K = 0, 2, \dots, l$  for even  $l$ , or  $K = 2, 4, \dots, (l-1)$  for odd  $l$ , compose the vector eigenfunction  $\Phi_{nl}$  corresponding to the eigenvalue  $E_n^l$  (in MeV) of the BVP for a system of  $l/2 + 1$  or  $(l-1)/2$  equations for even or odd  $l$ , respectively:

$$\left[ \hat{T}_{\text{vib}} + T'_{KK} + \frac{2}{\hbar^2} (V - E_{nl}) \right] \Phi_{nlK} + T'_{KK+2} \Phi_{nlK+2} + T'_{KK-2} \Phi_{nlK-2} = 0,$$

$$\hat{T}_{\text{vib}}(x_1, x_2) = -\frac{1}{g_0(x_1, x_2)} \sum_{i,j=1}^2 \frac{\partial}{\partial x_i} g_{ij}(x_1, x_2) \frac{\partial}{\partial x_j},$$

$$T'_{KK} = (l(l+1) - K^2) \left( \frac{1}{2J_1} + \frac{1}{2J_2} \right) + \frac{K^2}{J_3}, \quad T'_{KK\pm 2} = \left( \frac{1}{4J_1} - \frac{1}{4J_2} \right) C'_{KK\pm 2},$$

$$C'_{KK+2} = C'_{K+2K} = (1 + \delta_{K0})^{1/2} [(l-K)(l+K+1)(l-K-1)(l+K+2)]^{1/2},$$

$$J_k(x_1, x_2) = J_k(\beta, \gamma) = 4B_k(\beta, \gamma)\beta^2 \sin^2(\gamma - 2\pi k/3). \quad (10)$$

The components  $\Phi_{nlK}$  are subject to Neumann or Dirichlet boundary conditions at the boundary  $\partial\Omega_2$  of the domain  $\Omega_2$  and the orthogonality and normalization conditions

$$\int_0^{\beta_{\max}} \int_0^{\pi/3} g_0(\beta, \gamma) d\beta d\gamma \sum_{K \geq 0, \text{even}}^{l_{\max}} \Phi_{nlK}(\beta, \gamma) \Phi_{n'l'K}(\beta, \gamma) = \delta_{nn'}. \quad (11)$$

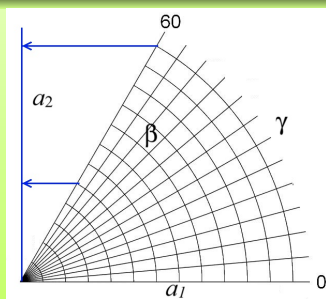
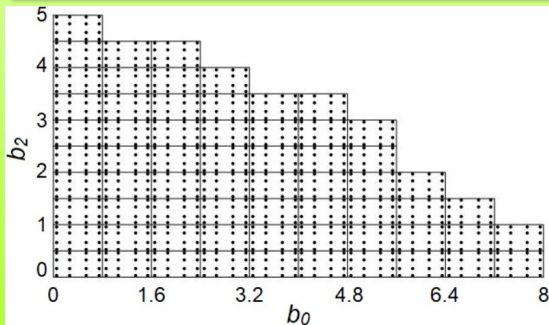
## Exact solvable 5D harmonic oscillator (5DHO)

$$V(\beta, \gamma) = (C_2/2)\beta^2, \quad B_{\beta\beta} = B_{\gamma\gamma} = B_1 = B_2 = B_3 = B_0, \quad B_{\beta\gamma} = B_{\gamma\beta} = 0,$$

$$g_0(\beta, \gamma) = B_0 g_{11}(\beta, \gamma) = B_0 \beta^2 g_{22}(\beta, \gamma) = B_0^{5/2} \beta^4 \sin(3\gamma), \quad g_{12}(\beta, \gamma) = g_{21}(\beta, \gamma) = 0.$$

Internal  $(a_0, a_2)$  and affine  $(b_0, b_2)$  coordinates

$$a_0 = \beta \cos(\gamma) = b_0 + \sqrt{\frac{2}{3}} b_2, \quad a_2 = \frac{1}{\sqrt{2}} \beta \sin(\gamma) = b_2.$$



Rectangular grid of finite elements for the 5D harmonic oscillator. The Gaussian nodes are marked by circles.

In grid  $\Omega_{b_0, b_2}$  the cells  $\Delta_q$  for which  $\min_{(b_0, b_2) \in \Delta_q} V(b_0, b_2) > 30$  are dropped.



## Theoretical estimations of the order of the 2d FEM scheme

The Runge coefficients  $R_h$  were calculated in the grids  $\Omega_{\beta,\gamma}$  and  $\Omega_{b_0,b_2}$

$$R_h = \log_2 \left| \frac{((E_n^I)_h - (E_n^I)_{h/2})}{((E_n^I)_{h/2} - (E_n^I)_{h/4})} \right|, \quad (12)$$

where  $(E_n^I)_h$ ,  $(E_n^I)_{h/2}$ ,  $(E_n^I)_{h/4}$  are the energies calculated by the program 2DFEM on the doubly condensed grids, gave estimates confirming the theoretical estimate of the order of  $2p'$  of the 2d FEM scheme.

The discrepancies  $\delta E_{l,n=1} = E_{l,n=1}^{\text{num}} - E_{l,n=1}$  of the eigenvalues  $E_{l,n=1}$  of the 5DHO model in coordinates  $(\beta, \gamma)$  (left panel) and  $(b_0, b_2)$  (right panel) and Runge coefficients (12) (Ru) by the FEM schemes with LIPs and HIPs of the order  $p' = 3$ .

$l$	$h$	$h/2$	$h/4$	Ru
0	5.4(-6)	9.2(- 8)	1.5(- 9)	5.88
2	9.6(-6)	1.6(- 7)	2.6(- 9)	5.92
3	1.4(-5)	4.2(- 7)	1.9(- 7)	5.93
0	1.4(-5)	2.8(- 7)	4.7(- 9)	5.62
2	2.2(-5)	4.7(- 7)	8.3(- 9)	5.57
3	2.9(-5)	1.2(- 6)	5.9(- 7)	5.47

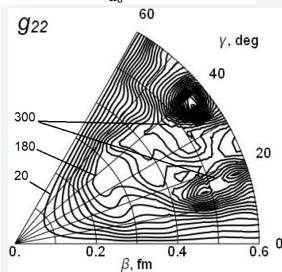
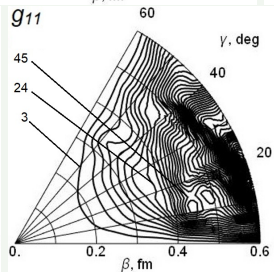
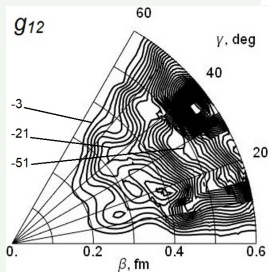
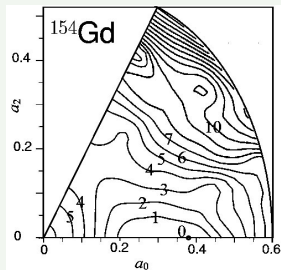
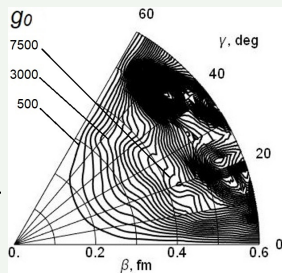
$l$	$h$	$h/2$	$h/4$	Ru
0	3.1(-4)	8.0(-6)	1.3(- 7)	5.28
2	9.2(-4)	1.5(-5)	2.6(- 7)	5.92
3	2.8(-3)	4.4(-5)	7.6(- 7)	6.03
0	4.8(-4)	1.8(-5)	3.9(- 7)	4.68
2	1.2(-3)	3.3(-5)	7.4(- 7)	5.20
3	3.3(-3)	8.6(-5)	2.1(- 6)	5.27

The calculations are performed at  $B_0 = 1$ ,  $C_2 = 1$ , and  $\hbar = 1$  on the grids

$\Omega_{\beta,\gamma} = [0(h_\beta)7] \otimes [0(h_\gamma)\pi/3]$  with  $h_\beta = h, h/2, h/4$  at  $h = 7/12$  and  $h_\gamma = \pi/(36)$  and  $\Omega_{b_0,b_2} = ([0(h_0)8] \otimes [0(h_2)5])$  with  $h_0 = h, h/2, h/4$ ,  $h_2 = 5h_0/8$  at  $h = 8/7$ .

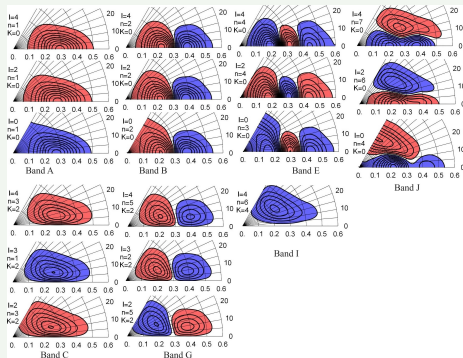
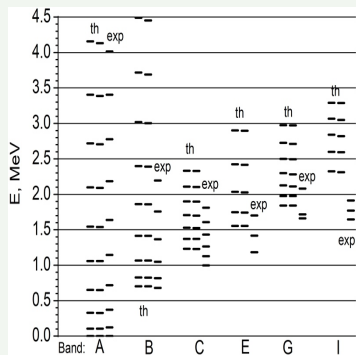
# Benchmark calculations of $^{154}\text{Gd}$ in the RMF model

Isolines of  $V(\beta, \gamma)$  counted from the minimum of  $V(\beta=0.3875, \gamma=0) = -1270.6\text{MeV}$ ,  $g_0(\beta, \gamma)$  and  $g_{ij}(\beta, \gamma)$  of  $^{154}\text{Gd}$  calculated in PC-F1 of RMF model



$$\hat{T}_{\text{vib}}(\beta, \gamma) = -\frac{1}{g_0(\beta, \gamma)} \sum_{i,j=1}^2 \frac{\partial}{\partial \beta} g_{ij}(\beta, \gamma) \frac{\partial}{\partial \gamma}$$

# Energy spectrum of $^{154}\text{Gd}$ and quasi-crossings of the energy bands



Energy spectrum of  $^{154}\text{Gd}$ . For each state of the bands A, B, E, C, G, and I, **three short bars correspond to the diagonal approximation (left), nondiagonal one (middle), and experiment (right)** [<http://www.nndc.bnl.gov/ensdf/>].

Band(A) is the  $K^\pi = 0^+$  ground state band;

Band(B): the first excited  $K^\pi = 0^+$  ( $\beta$ -vibrational) band;

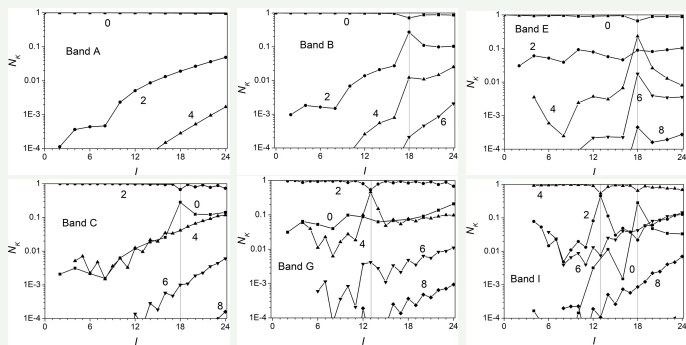
Band(E), Band(J), Band(K): the second, third and fourth excited  $K^\pi = 0^+$  bands;

Band(C): the  $K^\pi = 2^+$  ( $\gamma$ -vibrational) band;

Band(G): the second excited  $K^\pi = 2^+$  ( $\beta\gamma$ -vibrational) band;

Band(I): the  $K^\pi = 4^+$  band.

## Partial probability density integrals of components $\Phi_{nlK}(\beta, \gamma)$

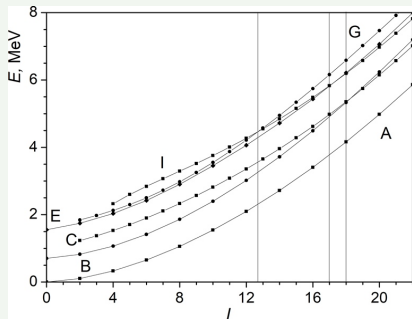


Integrals  $N_K \equiv N_{Kn}^l$  from Eq. (13) for each of A, B, E, C, G, and I bands at the values of  $K = 0, 2, 4, 6, 8$  labelling each of the curves.

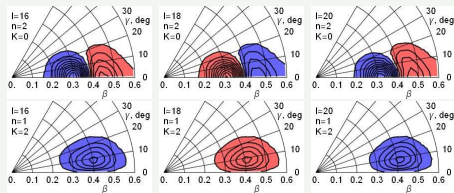
$$N_{Kn}^l = \int_0^{\beta_{\max}} \int_0^{\pi/3} g_0(\beta, \gamma) \Phi_{nlK}(\beta, \gamma) \Phi_{nlK}(\beta, \gamma) d\beta d\gamma, \quad \sum_{K \geq 0, \text{even}} N_{Kn}^l = 1. \quad (13)$$

The leading values of diagonal approximation do also confirm the experimental classification of each of A, B, E, C, G, and I bands, while a selected agreement with the experimental data is due to the above restriction of the model parametrization.

## Benchmark calculations of $^{154}\text{Gd}$ in the RMF model



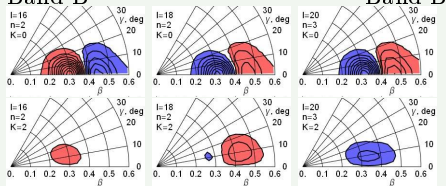
The lower part of the  $^{154}\text{Gd}$  spectrum in the diagonal and nondiagonal approximation for each of A, B, E, C, G, and I bands used in the experimental data tables  
<http://www.nndc.bnl.gov/ensdf/>



Isolines of the leading components  $\Phi_{nIK} = \pm 0.01, \pm 0.03, \dots$  of the  $^{154}\text{Gd}$  wave functions for  $n = 2, 3$  and  $I = 16, 18, 20$  in diagonal approximation.

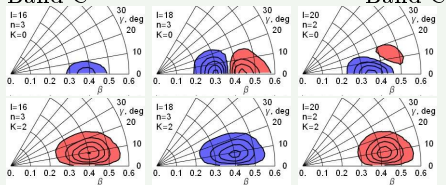
# Benchmark calculations of $^{154}\text{Gd}$ in the RMF model

## Band B



## Band B

## Band C

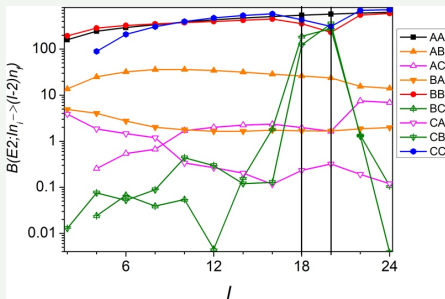


## Band C

Isolines of the leading components  $\Phi_{nlK} = \pm 0.01, \pm 0.03, \dots$  of the  $^{154}\text{Gd}$  wave functions for  $n = 2, 3$  and  $l = 16, 18, 20$  in **nondiagonal approximations**.

So, in the nondiagonal approximation at  $l = 16$  and  $l = 20$ , the leading components practically coincide with those in the diagonal approximation, and at  $l = 18$ , the components are their linear combinations, belonging to both bands.

## Calculated intraband and interband transitions



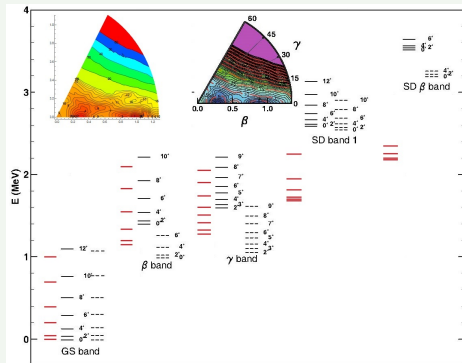
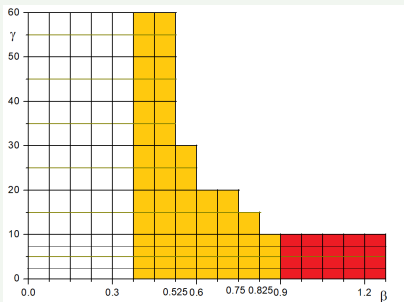
$B(E2)$	ndiag	diag	exp	bands
$2_1 \rightarrow 0_1$	160	159	157	AA
$4_1 \rightarrow 2_1$	244	243	245	
$6_1 \rightarrow 4_1$	294	293	285	
$8_1 \rightarrow 6_1$	341	339	312	
$10_1 \rightarrow 8_1$	387	385	360	
$2_2 \rightarrow 0_2$	194	193	97.0	BB
$0_2 \rightarrow 2_1$	68.5	69.2	52.0	BA
$2_2 \rightarrow 4_1$	45.0	45.5	19.6	
$2_3 \rightarrow 4_1$	0.460	0.248	1.72	CA
$2_3 \rightarrow 0_1$	3.89	4.14	5.70	

Calculated intraband and interband  $B(E2; I_n_i \rightarrow (I-2)n_f)$  transitions between A, B and C bands in Weisskopf units (W.u.) in the nondiagonal approximation (nondiag) for  $^{154}\text{Gd}$ .

In the vicinity of the quasi-crossing point at  $I = 18$ , the values of interband transitions between B and C bands are approximately 200 W.u., in comparison with small values ( $< 1$  W.u.) beyond the vicinity.

However, the intraband transitions in the B and C bands in the vicinity of the quasi-crossing point are approximately by two times smaller than beyond the vicinity.

# The potential energy surface and energy bands of $^{238}\text{U}$ in PC-PK1 RMF

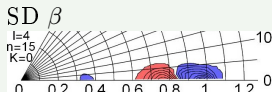
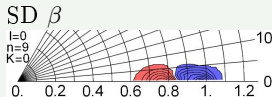
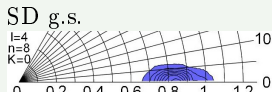
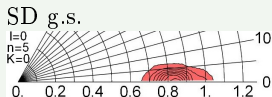
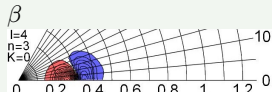
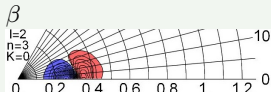
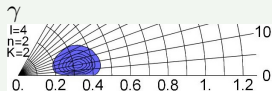
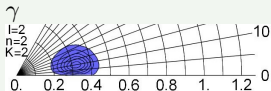
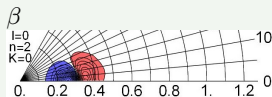
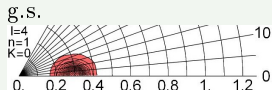
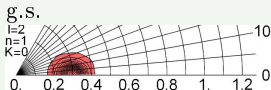
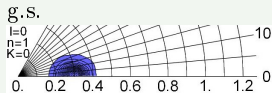


The 2d FEM grid and PES  $V(\beta, \gamma)$  using in calculations by 2DFEM program of the  $\pi = +$  energy levels  $E_{In}$  in the yrast and vibrational bands at normal and superdeformed shapes in  $^{238}\text{U}$  marked by red bars;

Experimental and calculated values from [Libert, J., Girod, M. and Delaroche, J.-P.L.: Microscopic descriptions of superdeformed bands with the Gogny forces: Configuration mixing calculations in the  $A \sim 190$  mass region, Phys. Rev. C 60, 054301-1-26 (1999)] are shown as black dotted and solid bars. The insert is for  $V(\beta, \gamma)$  in PC-PK1 RMF and in Gogny forces models.



# The leading components of eigenfunctions of $^{238}\text{U}$ in PC-PK1 RMF



The leading components of eigenfunctions of  $^{238}\text{U}$  in double well potential

## Conclusion

- To solve elliptic multidimensional BVPs, the high-precision FEM schemes using Hermite interpolation polynomials on parallelepipeds are elaborated and applied to solve the BVP arising in the collective models of atomic nuclei.
- The efficiency of the algorithms and programs is demonstrated by benchmark calculations of the lower part of the quadrupole rotational-vibrational spectrum of the 5DHO model.
- The 2DFEM program benchmark calculations in PC-F1 or PC-PK1 parametrizations of the self-consistent RMF model of  $^{154}\text{Gd}$  or  $^{238}\text{U}$  isotopes are in an agreement with the single or double GTM basis sets calculations for single or double potential wells.
- The calculations of the quadrupole spectrum  $E_{In}$  of  $^{154}\text{Gd}$  isotope and corresponding the reduced probabilities of electric interband and intraband  $B(E2)$  transitions for the model based on RMF revealed a possibility of quasi-crossing of energy levels belonging to different bands at some values of the nucleus spin.
- The developed approach and 2DFEM programs provide a base for adapting multidimensional FEM programs to solving the bound state problems of the rotational-vibrational spectrum, which are applicable in generalizations of the geometric quadrupole collective model, the self-consistent relativistic mean-field (RMF) model and the quadrupole-octupole six-dimensional collective model of atomic nuclei.

Thank you for your attention!